STM JOURNALS

Journal of
Polymer & Composites

ISSN: 2321-2810 (Online)
ISSN: 2321-8525 (Print)
Volume 12, Special, Issue 6, 2024
DOI (Journal): 10.37591/JoPC

https://journals.stmjournals.com/jopc

Research JoPC

Tb^{3+} Activated Boro Phosphate Glass: Synthesis and Photoluminescence (PL) Characteristics

U.A. Nage[1,*], C.S. Khade[2]

Abstract

The ($40B_2O_3$+ $3Al_2O_3$+(10-x) P_2O_5 + xTb + $7ZnO$+$5LiCO_3$+ $10H_6NO_4P$+$25SrCO_3$) boro phosphate glass was successfully synthesized via melt quenching method. The structural confirmation is supported with X-ray diffraction (XRD) data and surface morphology was defined by scanning electron microscope (SEM). The ($40B_2O_3$+ $3Al_2O_3$+(10-x) P_2O_5 + xTb+ $7ZnO$+$5LiCO_3$+ $10H_6NO_4P$+$25SrCO_3$) boro phosphate glass has been investigated for its Photoluminescence (PL) under UV excitation. At 544 nm, the excitation was observed, and at 222 nm, the emission was noted. After computation, the prepared glass's CIE (Commission International de l'Eclairage) coordinates were determined to be (x = 0.2585, y = 0.7305). Hence the ($40B_2O_3$+ $3Al_2O_3$+(10-x) P_2O_5 + xTb + $7ZnO$+$5LiCO_3$+ $10H_6NO_4P$+$25SrCO_3$)) boro phosphate glass has exhibit great potential as glass in green light-emitting diode (LED). The boro phosphate glass (40B2O3+ 3Al2O3+(10-x) P2O5 + xTb + 7ZnO+5LiCO3+ 10H6NO4P+25SrCO3) was synthesized using the melt quenching method and analyzed for structural and surface properties using XRD and SEM. Photoluminescence (PL) studies revealed excitation at 544 nm and emission at 222 nm under UV light. The CIE coordinates (x = 0.2585, y = 0.7305) confirm its suitability for green light-emitting applications. This material holds great promise for green LEDs, owing to its strong luminescent properties. The boro phosphate glass exhibits strong photoluminescence with excitation at 544 nm and emission at 222 nm. Its CIE coordinates confirm its potential for green LED applications.

Keywords: Green light-emitting diode, UV excitation Glass, X-ray diffraction, Phosphate, Terbium-doped glass

INTRODUCTION

Around the world, glass materials are essential to the realization of a wide range of applications, from lenses to optical fiber communication. They have a number of useful benefits, including easy mass manufacture at a low cost, diverse forms, and composition variation [1].

Glasses containing transition metal oxides have great interest in academic investigations and industrial applications. The optical properties of these glass matrices may be changed via addition of different transition metal oxide ratios [2].

***Author for Correspondence**
U.A. Nage
E-mail: umeshnage@gmail.com

[1]Lecturer ,Department of Science, Government Polytechnic, Washim, Maharashtra, India
[2]Assistant Professor, Department of Physics, GHRAET, Nagpur Maharashtra, India

Received Date: May 14, 2024
Accepted Date: July 20, 2024
Published Date: August 06, 2024

Citation: U.A. Nage, C.S. Khade. Tb^{3+} Activated Boro Phosphate Glass: Synthesis and Photoluminescence (PL) Characteristics. Journal of Polymer & Composites. 2024; 12(6): S43–S47p.

Glasses are frequently employed in the manufacturing of solid state lasers and have long been recognized as an appropriate host for REs.Glasses doped with rare earth ions have been widely examined and possess many advantages due to their laser action in visible and near infrared (NIR) regions that make them very considerable materials to be used as laser media and are currently best substitute to single crystals for all solid state laser emission [3].

Generally, the optical homogeneity of glassy matrices make available RE ions to exhibit diverse

latent laser transitions. Spectroscopic study of RE ions in glasses suggest information with consider to transition probabilities, lifetimes, branching ratios of the excited states, which are vital in the design and growth of diverse electro-optic and optical devices. Much research in the 1960s was concerned with the improvement of solid state lasers utilize the luminescence of RE ions in glasses and crystals. The Nd: YAG laser is probably the most central triumph from this period, and there is persistent interest in novel rare earth doped materials for lasers. All the rare earth ions (Pr^{3+}, Nd^{3+}, Sm^{3+}, Eu^{3+}, Gd^{3+}, Tb^{3+}, Dy^{3+}, Ho^{3+}, Er^{3+}, and Tm^{3+}) have their respective applications in the production of optical devices to extend advanced lasers and optical amplifiers to optoelectronic and optical communication applications in the field of rare earth (RE) luminescence.

More recently, however, optoelectronics has emerged as the principal area of research into RE luminescence, and the current article therefore focus on the different ways in which RE luminescence has been exploited in this field [4].

Throughout the last ten years, the area of rare-earth ion luminescence has grown steadily, mostly as a result of the growing need for optical sources and amplifiers that can operate at wavelengths that are compatible with fiber communications technology. Seldom used in optical fiber amplifiers, small micro chip lasers, planar waveguides, and solid state lasers, the 4f–4f electronic transitions of rare earth (RE) ions are significant.

In the present work, we have investigate the preparation and characterization of ($40B_2O_3$+ $3Al_2O_3$+(10-x) P_2O_5 + xTb + 7ZnO+$5LiCO_3$+ $10H_6NO_4P$+$25SrCO_3$) (x=0.001, 0.002,0.005,0.01 and 0.02) glass via melt quenching method.

EXPERIMENTAL

The Tb^{3+} activated Boro phosphate glasses with composition ($40B_2O_3$+ $3Al_2O_3$+(10-x) P_2O_5 + xTb + 7ZnO +$5LiCO_3$+ $10H_6NO_4P$+$25SrCO_3$) (x=0.001,0.002,0.005,0.01 and 0.02) were successfully prepared by melt quenching method.

X-ray diffraction (PXRD) was used to verify the phase purity of the produced photoshors. A Rigaku miniflex II diffractometer with Cu Kα (λ = 1.5405 Å) operating at 5 kV was used. Utilizing a 450W xenon lamp, the Hitachi F-7000 fluorescence spectrophotometer was used to detect the PL and PLE excitation spectra.

RESULTS AND DISCUSSION

X-Ray Diffraction (XRD) Pattern

The XRD pattern of prepared boro phosphate $40B_2O_3$+ $3Al_2O_3$+(10-x) P_2O_5 + xTb + 7ZnO +$5LiCO_3$+ $10H_6NO_4P$+$25SrCO_3$) glass as shown in Figure 1. From Figure 1 observed that the spectra have not shown any sharp peaks which indicate the amorphous nature of glass samples.

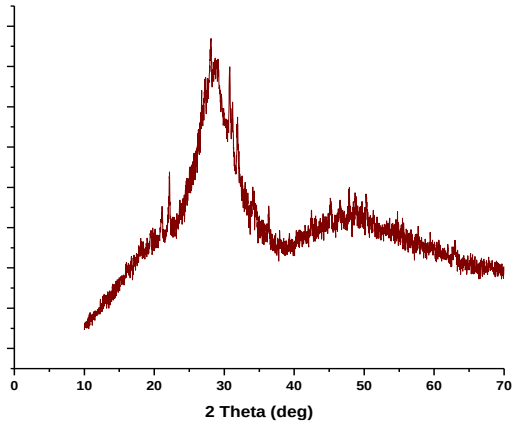

Figure 1. X-ray diffraction pattern of $40B_2O_3$+ $3Al_2O_3$+(10-x) P_2O_5 + xTb + 7ZnO +$5LiCO_3$+ $10H_6NO_4P$+$25SrCO_3$) glass

Surface morphology

Figure 2 shows the SEM image of Un-doped ($40B_2O_3$+$3Al_2O_3$+(10-x)P_2O_5+ +$7ZnO$+$5LiCO_3$+$10H_6NO_4P$+$25SrCO_3$) boro phosphate Glass. It is observed that the microstructure of the glass consist of irregular grains with light agglomeration. The average size of prepared glass is in submicron range.

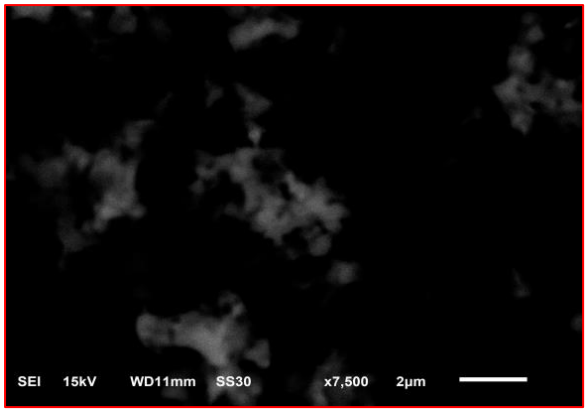

Figure 2. Surface morphology of prepared ($40B_2O_3$+$3Al_2O_3$+(10-x)P_2O_5 +$7ZnO$+$5LiCO_3$+$10H_6NO_4P$+$25SrCO_3$) Boro phosphate glass

Photoluminescence Properties (PL)

The excitation and emission spectra of ($40B_2O_3$+ $3Al_2O_3$ + (10-x) P_2O_5 + $_xTb^{3+}$ + $7ZnO$ + $5LiCO_3$+ $10H_6NO_4P$+$25SrCO_3$) (x= 0.001-0.02) glass was analyzed through fluorescence spectrophotometer at room temperature. Figure 3 displayed the excitation and emission spectra together. The excitation was observed under 544 nm and emission was observed under 222 nm. The wide band in the 200–250 nm range of the excitation spectrum corresponds to the Tb^{3+} transitions 4f–5d. The transition of Tb^{3+} is dominant in most of the materials. However, No charge-transfer (CT) transition related to Tb^{3+}–O^{2-} was observed, because it is located at much higher energy (60,000cm^{-1}) than the ^{5}d states of Tb^{3+} [5].

The emission spectrum consists of a series of sharp lines peak at 379 nm, 414 nm and 436 nm, corresponding to the $^5D_3$ to ^7F_J (J=6, 5, 4) transition of Tb^{3+} respectively. While, the peaks at 489, 544, 584 and 622 nm were corresponds to the $^5D_4$ to ^7F_J (J=6, 5, 4, 3) transitions within the $4f^8$ configurations Tb^{3+} [6]. The green emission lines between 490 to 630 nm are ascribed to the $^5D_4$ – ^7F_J (J =6, 5, 4, 3) transitions, while the blue emission lines from 380 to 480 nm are attributed to the $^5D_3$ transitions. \

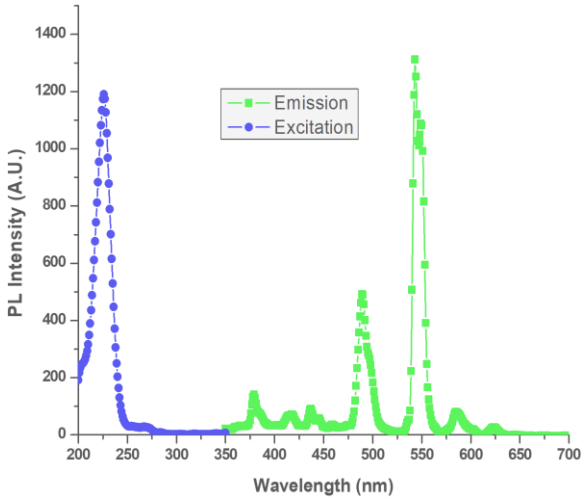

Figure 3. Photoluminescence excitation and emission spectra of ($40B_2O_3$+ $3Al_2O_3$ + (10-0.005) P_2O_5 + $_{0.005}Tb^{3+}$ + $7ZnO$ +$5LiCO_3$+ $10H_6NO_4P$+$25SrCO_3$) glass monitored at 544 nm and 222 nm

The Figure 4 showed emission spectra of ($40B_2O_3$+ $3Al_2O_3$ + (10-x) P_2O_5 + $_xTb^{3+}$ + 7ZnO + $5LiCO_3$+ $10H_6NO_4P$+$25SrCO_3$) glass doped with different concentration of Tb^{3+}. At first, the $^5D_3$ –^7F_J transitions is dominant with low doping concentrations in the emission spectra, and the $^5D_4$–$^7F_5$ transition at 544 nm plays an increasingly dominant role with enhancing the doping concentrations. The quenching of the blue emissions of $^5D_3$–^7F_J transitions is due to the cross-relaxation between the $^5D_3$–$^5D_4$ and $^7F_0$–$^7F_6$ of the two adjacent Tb^{3+} ions. In addition, the green emissions of the $^5D_4$ –^7F_J transitions are quenched via the energy migration between the activators [7–10].

Figure 4 represents emission spectra of ($40B_2O_3$+ $3Al_2O_3$ + (10-x) P_2O_5 + $_xTb^{3+}$ + 7ZnO + $5LiCO_3$+ $10H_6NO_4P$+$25SrCO_3$) glass doped with different concentration Tb^{3+} and observed that PL intensity was optimum at 0.005 mol of Tb ion.

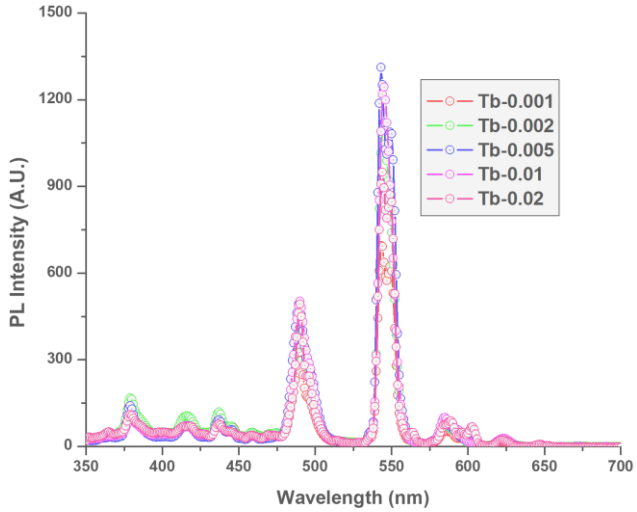

Figure 4. Photoluminescence emission spectra for various concentration of Tb^{3+} in ($40B_2O_3$+ $3Al_2O_3$ + (10-X) P_2O_5 + xRE^{3+}+ 7ZnO +$5LiCO_3$+ $10H_6NO_4P$+$25SrCO_3$) glass monitored at 222 nm

Photometric Characterization

Figure 5 Displays the color coordinates for ($40B_2O_3$+ $3Al_2O_3$ + (10-0.005) P_2O_5 + $_{0.005}Tb^{3+}$ + 7ZnO +$5LiCO_3$+ $10H_6NO_4P$+$25SrCO_3$) boro-phosphate glass compute by radiant imaging software based on the standard formulations made available by CIE (Commission International de I' Eclairage, France) which recognize that the human being visual system uses three color (red, green and blue).

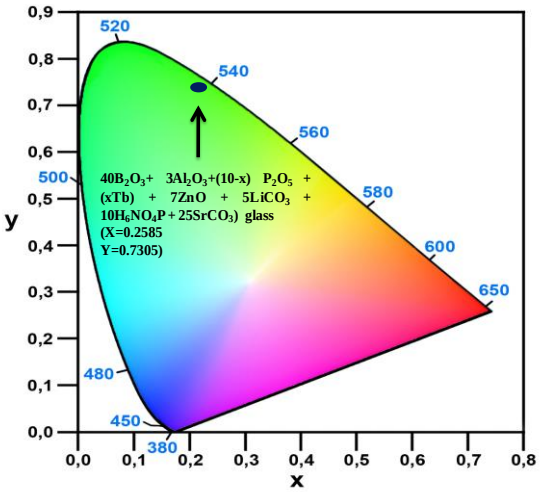

Figure 5. CIE chromaticity diagram of ($40B_2O_3$+ $3Al_2O_3$ + (10-X) P_2O_5 + xRE^{3+}+ 7ZnO +$5LiCO_3$+ $10H_6NO_4P$+$25SrCO_3$) (RE=Tb^{3+})

CIE coordinates of ($40B_2O_3$+ $3Al_2O_3$ + (10-X) P_2O_5 + xRE^{3+}+ 7ZnO +$5LiCO_3$+ $10H_6NO_4P$+$25SrCO_3$) (RE=Tb^{3+}) was measured as (x = 0.2585, y = 0.7305). The location of coordinate has been marked in Figure 4. with a black circle.

CONCLUSIONS

The ($40B_2O_3$+ $3Al_2O_3$+(10-x) P_2O_5 + xTb + 7ZnO +$5LiCO_3$+ $10H_6NO_4P$+$25SrCO_3$) (x=0.001,0.002,0.005,0.01 and 0.02) boro phosphate glass were successfully synthesized by melt quenching method. The XRD patterns of ($40B_2O_3$+ $3Al_2O_3$+(10-0.001) P_2O_5 + $_{0.001}$Tb + 7ZnO +$5LiCO_3$+ $10H_6NO_4P$+$25SrCO_3$) borate glass is similar in shape with Un-doped $40B_2O_3$+ $3Al_2O_3$ + (10) P_2O_5 + 7ZnO +$5LiCO_3$+ $10H_6NO_4P$+$25SrCO_3$ borate glass and observed that the spectra have not shown any sharp peaks which indicate the amorphous nature of glass samples.

Monitoring of the PL excitation spectrum took place at 544 nm, whereas emission was observed at 222 nm. The PL emission spectra observed that 0.005 mol is the optimum concentration for the prepared borate glass. The glass as prepared has the following CIE chromaticity coordinates: (x = 0.2585, y = 0.7305). The results indicate that $40B_2O_3$+ $3Al_2O_3$ + (10-x) P_2O_5 + xTb^{3+}+ 7ZnO +$5LiCO_3$+ $10H_6NO_4P$+$25SrCO_3$ borate glass is a prospective candidate for green emitting lighting.

Acknowledgement

One of the authors UAN is very much thankful to Head, Department of Physics S.G.B. Amravati University, Amravati for providing the necessary facilities for the analysis of XRD and PL results.

REFERENCES

1. Fujino S, Morinaga K. Structural analysis of glassy alloys containing rare earth metals. Eng Sci Rep Kyushu Univ. 1980;19(2):179–185.
2. Taha TA, Abouhaswa AS. Synthesis and characterization of novel nanocomposites for electronic applications. J Mater Sci Mater Electron. 2018. Available from: https://doi.org/10.1007/s10854–018-8816-7.
3. Koechner W. Solid state laser engineering. 3rd ed. Berlin: Springer; 2006.
4. Reddy CM, Raju BDP, Sushma NJ, Dhoble NS, Dhoble SJ. Review on the energy storage performance of different photovoltaic systems. Renew Sustain Energy Rev. 2015;51:566.
5. Bajaj NS, Omanwar SK. Luminescence properties of phosphor materials for white LED applications. J Lumin. 2014;153:288.
6. Bajaj NS, Palan CB, Omanwar SK. Structural and optical properties of doped nanophosphors for solid-state lighting. Int J Mater Sci Eng. 2015;3:167.
7. Zeng C, Hu Y, Xia Z, Huang H. Synthesis and luminescent properties of rare earth doped phosphors for LED applications. RSC Adv. 2015;5:68099.
8. Palaspagar R, Gawande A, Sonekar R, Omanwar S. Synthesis and characterization of novel phosphors for lighting applications. J Chin Adv Mater Soc. 2015;3:170.
9. Palaspagar R, Gawande A, Sonekar R, Omanwar S. Enhanced luminescence properties of novel phosphor materials for display applications. Mater Res Bull. 2015;72:215.'
10. Palan, C.B., Koparkar, K.A., Bajaj, N.S. et al. Synthesis and thermoluminescence/optically stimulated luminescence properties of CaB4O7:Ce phosphor. J Mater Sci: Mater Electron 27, 5600–5606 (2016). https://doi.org/10.1007/s10854-016-4465-x

